Sliding Mode Observers for Systems with Unknown Inputs: Application to estimate the Road Profile

H Imine, Kouider Nacer M'Sirdi, Y Delanne

Sliding-mode observers for systems with unknown inputs: application to estimating the road profile

H Imine[1*,2], **N K M'Sirdi**[1], and **Y Delanne**[2]
[1]Laboratoire de Robotique de Versailles, Velizy, France
[2]Laboratoire Central des Ponts et Chaussées, Bouguenais, France

Abstract: In this paper, a sliding-mode observer for systems with unknown inputs is presented. The system considered is a vehicle model with unknown inputs that represent the road profile variations. Coefficients of road adhesion are considered as unknown parameters. The tyre–road friction depends essentially on these parameters. The developed observer permits these longitudinal forces acting on the wheels to be estimated. Then another observer is developed to estimate the unknown inputs. In the first part of this work, some results are presented which are related to the validation of a full-car modelization, by means of comparisons between simulations results and experimental measurements (from a Peugeot 406 as a test car).

Keywords: road profile, tyre–road friction, vehicle modelling, sliding-mode observers

1 INTRODUCTION

Road profile unevenness through road–vehicle dynamic interaction and vehicle vibration affects safety (tyre contact forces), ride comfort, energy consumption, and wear. The road profile unevenness is consequently basic information for road maintenance management systems [**1**]. In order to obtain this road profile, several methods have been developed. Measurement of road roughness has been the subject of numerous research studies for more than 70 years [**2–5**]. Methods developed can be classified in two types: the response type and the profiling method. Nowadays the profiling method, which gives a road profile along a measuring line, is generally preferred. These methods pertain to two basic techniques: the rolling-beam or the inertial profiling method. The latter method, which was first proposed in 1964 [**6**], is now used worldwide. Inertial profiling methods consist in analysing the signal coming from displacement sensors and accelerometers [**5**, **7**]. One problem with the inertial profiling method, as currently used, is the impossibility of building up a three-dimensional profile from the elementary measurements needed for a road–vehicle interaction simulation package. It is worthwhile to mention that these methods do not take into consideration the dynamic behaviour of the vehicle. However, it has been shown that modifications of the dynamic behaviour may lead to biased results.

Finding a way to obtain a three-dimensional profile from the dynamic response of an instrumented car driven on a chosen road section is the general purpose of research engaged in at the Laboratoire Central des Ponts et Chaussées (LCPC) in cooperation with the Laboratoire de Robotique de Versailles.

The method proposed estimates the unknown inputs of the system corresponding to the height of the road by the use of sliding-mode observers [**8–12**].

The design of such observers requires a dynamic model. In the first step, a model is built up for a vehicle [**13**]. This model has been experimentally validated by comparing the estimated and measured dynamics responses of a Peugeot 406 vehicle (as a test car). The longitudinal forces which depend on the road adhesion coefficients are estimated with a sliding-mode observer [**14**].

* *Corresponding author: Laboratoire de Robotique de Versailles, UVSQ CNRS FRE 2659, Laboratoire Central des Ponts et Chaussées, 10 Avenue de l'Europe, Velisy, 78140, France. email: imine@robot.uvsq.fr*

Section 2 of this paper deals with the vehicle description and modelling. Section 3 is devoted to some comparison results to evaluate the accuracy of the full-car model. Then the observer design is presented in section 4. The main results are presented in section 5 to show the accuracy of the estimated road profile coming from the observer-based method. Finally, section 6 concludes on the effectiveness of the method.

2 VEHICLE DYNAMIC MODEL

When considering the vertical displacement along the z axis, the dynamic model of the system can be written as

$$\mathbf{M}\ddot{\boldsymbol{q}} + \mathbf{B}\dot{\boldsymbol{q}} + \mathbf{K}\boldsymbol{q} + \boldsymbol{G} = \mathbf{C}\boldsymbol{U} + \mathbf{D}\dot{\boldsymbol{U}} \tag{1}$$

$\boldsymbol{q} \in \Re^8$ is the coordinates vector defined by

$$\boldsymbol{q} = [z_1, z_2, z_3, z_4, z, \theta, \phi, \psi]^{\mathrm{T}} \tag{2}$$

where $(\dot{\boldsymbol{q}}, \ddot{\boldsymbol{q}})$ represent the vectors of the velocities and accelerations respectively. $\boldsymbol{G}$ is related to the gravity effects, $\boldsymbol{U} = (u_1, u_2, u_3, u_1)^{\mathrm{T}}$ is the vector of unknown inputs which characterize the road profile, the matrices **C** and **D** are functions of spring stiffness and damping respectively. **M** is the inertia matrix, **B** is related to the damping effects, and **K** is the spring stiffness matrix (Fig. 1).

A dynamic model of the vehicle can be defined as

$$m\begin{bmatrix} \dot{v}_x \\ \dot{v}_y \\ \dot{v}_z \end{bmatrix} = \boldsymbol{F} \tag{3}$$

where $\boldsymbol{v} = [v_x, v_y, v_z]^{\mathrm{T}}$ is the vector of the vehicle velocities (along the $\boldsymbol{x}$, $\boldsymbol{y}$ and $\boldsymbol{z}$ axes respectively) and $\boldsymbol{F}$ is the vector of the tyre-road frictional forces. By assuming that the longitudinal forces are proportional to the transverse forces, these forces can be expressed as

$$F_{xf} = \mu F_{zf} \tag{4}$$

where F_{zfi} and F_{zri}, $i = 1, \ldots, 2$, are the vertical forces of the front and rear wheels respectively. F_{xfi} and F_{xri}, $i = 1, \ldots, 2$, represent the longitudinal forces of the front and rear wheels respectively.

Figure 2 represents the variations in the road adhesion μ with respect to the longitudinal slip λ.

Many researchers have proposed different methods to measure these two coefficients. Bakker *et al.* [**15**] proposed 'a magic formula'. In the linear area of Fig. 2

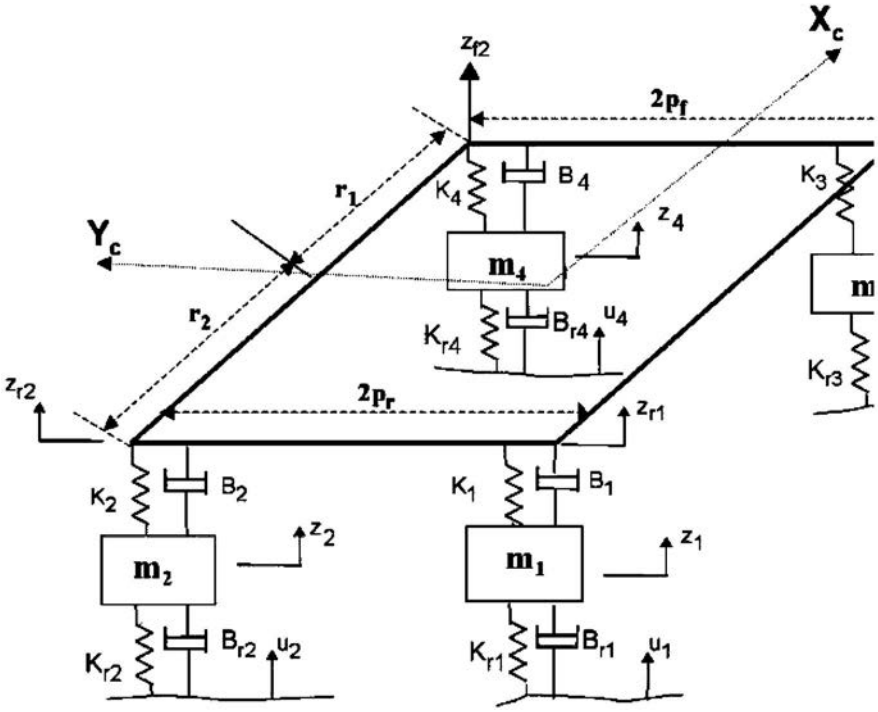

Fig. 1 Vehicle model

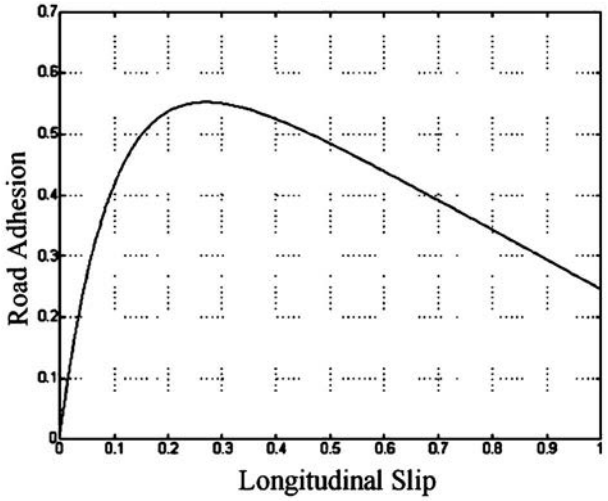

Fig. 2 Variations in the road adhesion with longitudinal slip

(longitudinal slip between 0 and 0.1), Burkhardt [**16**] simplified the model of tyre–road contact as

$$\mu = C_1[1 - \exp(-C_2\lambda)] - C_3\lambda \tag{5}$$

where C_1, C_2, and C_3 represent the pneumatic parameters. The longitudinal slip λ is defined by

$$\lambda = \left| \frac{v_r - v_x}{\max(v_r, v_x)} \right| \tag{6}$$

where v_r is the wheel velocity.

Figure 3 represents the longitudinal slip during the test reported here at a speed of 20 m/s.

It should be noted that this longitudinal slip is located in the linear area (longitudinal slip is between 0 and 0.1; see Fig. 2). Therefore, this justifies the use of the Burkhardt model in this work.

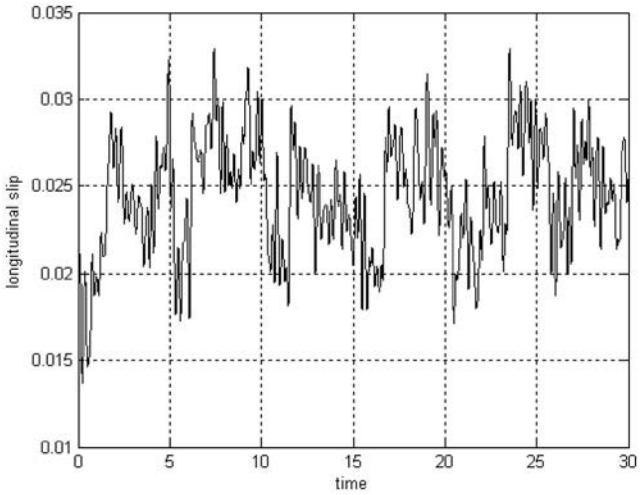

Fig. 3 Longitudinal slip during the test

The wheel angular motion is given by

$$\begin{aligned} J_{\mathrm{fi}}\dot{\omega}_{\mathrm{fi}} &= T_{\mathrm{ei}} - rF_{x\mathrm{fi}} \\ J_{\mathrm{ri}}\dot{\omega}_{\mathrm{ri}} &= -rF_{x\mathrm{ri}} \end{aligned} \tag{7}$$

where T_{ei}, $i = 1, 2$, is the engine torque, r is the wheel radius, and J_{fi} and J_{ri} are the wheel inertias.

Remark 1

The engine torque is deduced using the vehicle speed and the throttle position, without an explicit model for the engine behaviour. The steering and braking angles, the braking torque, and rolling resistance are measured.

3 ESTIMATION OF THE ROAD PROFILE

In this section, the sliding-mode observers are developed to estimate the unknown inputs of the system and the longitudinal forces [**17–20**]. The vertical dynamic model (1) can be written in the state form as

$$\begin{aligned} \dot{\boldsymbol{x}} &= f(\boldsymbol{x}) + \mathbf{C}\boldsymbol{U} + \mathbf{D}\dot{\boldsymbol{U}} \\ \boldsymbol{y} &= h(\boldsymbol{x}) \end{aligned} \tag{8}$$

where the state vector $\boldsymbol{x} = (\boldsymbol{x}_{11}, \boldsymbol{x}_{12})^{\mathrm{T}} = (\boldsymbol{q}, \dot{\boldsymbol{q}})^{\mathrm{T}}$, and $\boldsymbol{y} = \boldsymbol{q}(\boldsymbol{y} \in \Re^8)$ is the vector of measured outputs of the system.

Thus,

$$\begin{aligned} \dot{\boldsymbol{x}}_{11} &= \boldsymbol{x}_{12} \\ \dot{\boldsymbol{x}}_{12} &= \mathbf{M}^{-1}(-\mathbf{B}\boldsymbol{x}_{12} - \mathbf{K}\boldsymbol{x}_{11} - \boldsymbol{G}) + \mathbf{M}^{-1}(\mathbf{C}\boldsymbol{x}_3 + \mathbf{D}\boldsymbol{x}_4) \\ \dot{\boldsymbol{x}}_3 &= \boldsymbol{x}_4 \\ \dot{\boldsymbol{x}}_4 &= \mathbf{0} \end{aligned} \tag{9}$$

where $\boldsymbol{x}_3 = \boldsymbol{U}$.

Before developing the sliding-mode observer, the following assumptions must be considered.

1. The state is bounded ($\|\boldsymbol{x}(t)\| < \infty$, $\forall\, t \geqslant 0$).
2. The system is inputs bounded ($\exists$ a constant $\boldsymbol{\mu} \in \Re^4$ such that: $\dot{\boldsymbol{U}} < \boldsymbol{\mu}$).
3. The vehicle rolls at constant speed on a defect road of the order of millimetres, without bumps. It can then be assumed that $\ddot{\boldsymbol{U}} = \mathbf{0}$.

In the state form, the wheel angular motion becomes

$$\begin{aligned}\dot{\xi}_1 &= \xi_2 = \mathbf{J}^{-1}(\boldsymbol{\Gamma} - \mathbf{R}\boldsymbol{\Psi})\\ \boldsymbol{y}_1 &= \xi_1\end{aligned} \tag{10}$$

$\xi = (\xi_1, \xi_2)^{\mathrm{T}}$ where $\xi_1 = \boldsymbol{y}_1 = [\omega_{\mathrm{r1}}, \omega_{\mathrm{r2}}, \omega_{\mathrm{f1}}, \omega_{\mathrm{f2}}]^{\mathrm{T}}$ represents the measured angular velocity vector and ξ_2 is the vector of angular accelerations.

Because of small variations in the longitudinal forces, it is assumed that $\dot{\boldsymbol{\Psi}} = \mathbf{0}$,

$$\mathbf{J} = \begin{bmatrix} J_{\mathrm{r1}} & 0 & 0 & 0 \\ 0 & J_{\mathrm{r2}} & 0 & 0 \\ 0 & 0 & J_{\mathrm{f1}} & 0 \\ 0 & 0 & 0 & J_{\mathrm{f2}} \end{bmatrix}$$

$\boldsymbol{\Gamma} = [0,\ 0,\ T_{\mathrm{e1}},\ T_{\mathrm{e2}}]^{\mathrm{T}}$, $\mathbf{R} = r * \boldsymbol{\lambda}$ (with $\boldsymbol{\lambda} \in \Re^{4\times 4}$ is the identity matrix) and $\boldsymbol{\Psi} = [F_{xr1}, F_{xr2}, F_{xf1}, F_{xf2}]^{\mathrm{T}}$ represents the vector of the longitudinal forces to be estimated.

3.1 Observer design

In order to estimate the state vector $\boldsymbol{x}$ and to deduce both the unknown inputs vector $\boldsymbol{U}$ and its derivative $\dot{\boldsymbol{U}}$, the sliding mode observer:

$$\begin{aligned}\dot{\hat{\boldsymbol{x}}}_{11} &= \hat{\boldsymbol{x}}_{12} + \mathbf{H}_1 \operatorname{sgn}(\tilde{\boldsymbol{x}}_{11})\\ \dot{\hat{\boldsymbol{x}}}_{12} &= -\mathbf{M}^{-1}(\mathbf{B}\hat{\boldsymbol{x}}_{12} + \mathbf{K}\hat{\boldsymbol{x}}_{11} + \boldsymbol{G})\\ &\quad + \mathbf{M}^{-1}(\mathbf{C}\hat{\boldsymbol{x}}_3 + \mathbf{D}\hat{\boldsymbol{x}}_4) + \mathbf{H}_2 \operatorname{sgn}(\tilde{\boldsymbol{x}}_{11})\\ \dot{\hat{\boldsymbol{x}}}_3 &= \hat{\boldsymbol{x}}_4 + \mathbf{H}_3 \operatorname{sgn}(\tilde{\boldsymbol{x}}_{11})\\ \dot{\hat{\boldsymbol{x}}}_4 &= \mathbf{H}_4 \operatorname{sgn}(\tilde{\boldsymbol{x}}_{11})\end{aligned} \tag{11}$$

is proposed, where $\hat{\boldsymbol{x}}_{11} = \boldsymbol{x}_{11} - \hat{\boldsymbol{x}}_{11}$ is the state estimation error. $\mathbf{H}_1 \in \Re^{8\times 8}$ and $\mathbf{H}_2 \in \Re^{8\times 8}$ represent positive diagonal gain matrices. $\mathbf{H}_3 \in \Re^{4\times 8}$ and $\mathbf{H}_4 \in \Re^{4\times 8}$ are the gain matrices. Let us now define another observer to estimate the vector $\boldsymbol{\Psi}$ of longitudinal forces. It has the form

$$\begin{aligned}\dot{\hat{\xi}}_1 &= \mathbf{J}^{-1}(\boldsymbol{\Gamma} - \mathbf{R}\hat{\boldsymbol{\Psi}}) + \boldsymbol{\Lambda}_1 \operatorname{sgn}(\tilde{\xi}_1)\\ \dot{\hat{\boldsymbol{\Psi}}} &= \boldsymbol{\chi} + \boldsymbol{\Lambda}_2 \operatorname{sgn}(\tilde{\xi}_1)\end{aligned} \tag{12}$$

where $\boldsymbol{\Lambda}_1 \in \Re^{4\times 4}$ and $\boldsymbol{\Lambda}_2 \in \Re^{4\times 4}$ represent positive diagonal gain matrices. $\boldsymbol{\chi}$ is used to increase the robustness of the observer.

3.2 Convergence analysis

The dynamics estimation errors can be written as

$$\begin{aligned}\dot{\tilde{\boldsymbol{x}}}_{11} &= \tilde{\boldsymbol{x}}_{12} - \mathbf{H}_1 \operatorname{sgn}(\tilde{\boldsymbol{x}}_{11})\\ \dot{\tilde{\boldsymbol{x}}}_{12} &= -\mathbf{M}^{-1}(\mathbf{B}\tilde{\boldsymbol{x}}_{12} + \mathbf{K}\tilde{\boldsymbol{x}}_{11})\\ &\quad + \mathbf{M}^{-1}\mathbf{C}\tilde{\boldsymbol{x}}_3 + \mathbf{M}^{-1}\mathbf{D}\tilde{\boldsymbol{x}}_4 - \mathbf{H}_2 \operatorname{sgn}(\tilde{\boldsymbol{x}}_{11})\\ \dot{\tilde{\boldsymbol{x}}}_3 &= \tilde{\boldsymbol{x}}_4 - \mathbf{H}_3 \operatorname{sgn}(\tilde{\boldsymbol{x}}_{11})\\ \dot{\tilde{\boldsymbol{x}}}_4 &= -\mathbf{H}_4 \operatorname{sgn}(\tilde{\boldsymbol{x}}_{11})\end{aligned} \tag{13}$$

In order to study the observer stability and to find the gain matrices $\mathbf{H}_i$, $i = 1, \ldots, 4$, firstly, the convergence of $\tilde{\boldsymbol{x}}_{11}$ to the sliding surface $\tilde{\boldsymbol{x}}_{11} = \mathbf{0}$, in finite time t_1, must be proved. Then, some conditions about $\tilde{\boldsymbol{x}}_{12}$ must be deduced to ensure its convergence towards $\mathbf{0}$. Finally, it must be proved that the input estimation errors (namely $\tilde{\boldsymbol{x}}_3$ and $\tilde{\boldsymbol{x}}_4$) converge towards $\mathbf{0}$.

Consider the Lyapunov function

$$V_1 = \tfrac{1}{2}\tilde{\boldsymbol{x}}_{11}^{\mathrm{T}}\tilde{\boldsymbol{x}}_{11} \tag{14}$$

The time derivative of this function is given by

$$\dot{V}_1 = \tilde{\boldsymbol{x}}_{11}^{\mathrm{T}}[\tilde{\boldsymbol{x}}_{12} - \mathbf{H}_1 \operatorname{sgn}(\tilde{\boldsymbol{x}}_{11})] \tag{15}$$

By considering the gains matrix $\mathbf{H}_1 = \operatorname{diag}(h_{i1})$ with $h_{i1} > |\tilde{\boldsymbol{x}}_{i2}|$, $i = 1, \ldots, 8$, then $\dot{V}_1 < 0$. Therefore, from sliding-mode theory [**21**], the surface defined by $\tilde{\boldsymbol{x}}_{11} = \mathbf{0}$ is attractive, leading $\hat{\boldsymbol{x}}_{11}$ to converge towards $\boldsymbol{x}_{11}$ in finite time t_0. Moreover, $\dot{\tilde{\boldsymbol{x}}} = \mathbf{0}\ \forall\ t \geqslant t_0$. Consequently and according to equation (13), for $t \geqslant t_0$,

$$\operatorname{sgn}_{\mathrm{eq}}(\tilde{\boldsymbol{x}}_{11}) = \mathbf{H}_1^{-1}\tilde{\boldsymbol{x}}_{12} \tag{16}$$

where $\operatorname{sgn}_{\mathrm{eq}}$ represents an equivalent form of the sgn function on the sliding surface. Then the equation system (13) can be written as

$$\begin{aligned}\dot{\tilde{\boldsymbol{x}}}_{11} &= \tilde{\boldsymbol{x}}_{12} - \mathbf{H}_1 \operatorname{sgn}_{\mathrm{eq}}(\tilde{\boldsymbol{x}}_{11}) \to \mathbf{0}\\ \dot{\tilde{\boldsymbol{x}}} &= -\mathbf{M}^{-1}\mathbf{B}\tilde{\boldsymbol{x}}_{12} + \mathbf{M}^{-1}\mathbf{C}\tilde{\boldsymbol{x}}_3 + \mathbf{M}^{-1}\mathbf{D}\tilde{\boldsymbol{x}}_4 - \mathbf{H}_2\mathbf{H}_1^{-1}\tilde{\boldsymbol{x}}_{12}\\ \dot{\tilde{\boldsymbol{x}}}_3 &= \tilde{\boldsymbol{x}}_4 - \mathbf{H}_3\mathbf{H}_1^{-1}\tilde{\boldsymbol{x}}_{12}\\ \dot{\tilde{\boldsymbol{x}}}_4 &= -\mathbf{H}_4\mathbf{H}_1^{-1}\tilde{\boldsymbol{x}}_{12}\end{aligned} \tag{17}$$

By considering the matrix $\mathbf{H}_3$ components $(h_{i3},\ i = 1, \ldots, 4)$ such that $h_{i3} > |\tilde{\boldsymbol{x}}_{i4}|$, then the equation system (17) becomes, for $t \geqslant t_0$,

$$\begin{aligned}\dot{\tilde{\boldsymbol{x}}}_{11} &= \mathbf{0}\\ \dot{\tilde{\boldsymbol{x}}}_{12} &= -\mathbf{M}^{-1}\mathbf{B}\tilde{\boldsymbol{x}}_{12} + \mathbf{M}^{-1}\mathbf{C}\tilde{\boldsymbol{x}}_3 + \mathbf{M}^{-1}\mathbf{D}\tilde{\boldsymbol{x}}_4 - \mathbf{H}_2\mathbf{H}_1^{-1}\tilde{\boldsymbol{x}}_{12}\\ \dot{\tilde{\boldsymbol{x}}} &= -\mathbf{H}_3\mathbf{H}_1^{-1}\tilde{\boldsymbol{x}}_{12}\\ \dot{\tilde{\boldsymbol{x}}} &= -\mathbf{H}_4\mathbf{H}_1^{-1}\tilde{\boldsymbol{x}}_{12}\end{aligned} \tag{18}$$

Now, consider a (second) Lyapunov function V_2 and its time derivative $\dot{V}_2$ given by

$$\begin{aligned} V_2 &= \tfrac{1}{2}\tilde{\boldsymbol{x}}_{12}^{\mathrm{T}}\mathbf{M}\tilde{\boldsymbol{x}}_{12} + \tfrac{1}{2}\tilde{\boldsymbol{x}}_3^{\mathrm{T}}\mathbf{P}_1\tilde{\boldsymbol{x}}_3 + \tfrac{1}{2}\tilde{\boldsymbol{x}}_4^{\mathrm{T}}\mathbf{P}_2\tilde{\boldsymbol{x}}_4 \\ \dot{V}_2 &= \tilde{\boldsymbol{x}}_{12}^{\mathrm{T}}\mathbf{M}\dot{\tilde{\boldsymbol{x}}}_{12} + \tilde{\boldsymbol{x}}_3^{\mathrm{T}}\mathbf{P}_1\dot{\tilde{\boldsymbol{x}}}_3 + \tilde{\boldsymbol{x}}_4^{\mathrm{T}}\mathbf{P}_2\dot{\tilde{\boldsymbol{x}}}_4 \end{aligned} \tag{19}$$

where $\mathbf{P}_1 \in \Re^{4\times 4}$ and $\mathbf{P}_2 \in \Re^{4\times 4}$ are positive diagonal gain matrices. Then, from equation (17), $\dot{V}_2$ becomes

$$\begin{aligned} \dot{V}_2 = &-\tilde{\boldsymbol{x}}_{12}^{\mathrm{T}}\mathbf{B}\tilde{\boldsymbol{x}}_{12} - \tilde{\boldsymbol{x}}_{12}^{\mathrm{T}}\mathbf{M}\mathbf{H}_2\mathbf{H}_1^{-1}\tilde{\boldsymbol{x}}_{12} + \tilde{\boldsymbol{x}}_{12}^{\mathrm{T}}\mathbf{C}\tilde{\boldsymbol{x}}_3 + \tilde{\boldsymbol{x}}_{12}^{\mathrm{T}}\mathbf{D}\tilde{\boldsymbol{x}}_4 \\ &-\tilde{\boldsymbol{x}}_3^{\mathrm{T}}\mathbf{P}_1\mathbf{H}_3\mathbf{H}_1^{-1}\tilde{\boldsymbol{x}}_{12} - \tilde{\boldsymbol{x}}_4^{\mathrm{T}}\mathbf{P}_2\mathbf{H}_4\mathbf{H}_1^{-1}\tilde{\boldsymbol{x}}_{12} \end{aligned} \tag{20}$$

By considering that $\mathbf{H}_3$ and $\mathbf{H}_4$ are such that

$$\begin{aligned} \mathbf{P}_1\mathbf{H}_3\mathbf{H}_1^{-1} &= \mathbf{C}^{\mathrm{T}} \\ \mathbf{P}_2\mathbf{H}_4\mathbf{H}_1^{-1} &= \mathbf{D}^{\mathrm{T}} \end{aligned} \tag{21}$$

finally it is found that

$$\dot{V}_2 = -\tilde{\boldsymbol{x}}_{12}^{\mathrm{T}}(\mathbf{B} + \mathbf{M}\mathbf{H}_2\mathbf{H}_1^{-1})\tilde{\boldsymbol{x}}_{12} \tag{22}$$

Recalling that $\mathbf{M}$ and $\mathbf{H}_1$ are positive definite matrices, and by choosing $\mathbf{H}_2$ of the form

$$\mathbf{H}_2 = \mathbf{M}^{-1}(\mathbf{Q} - \mathbf{B})\mathbf{H}_1 \tag{23}$$

such that $\mathbf{Q} = \mathbf{B} + \mathbf{M}\mathbf{H}_2\mathbf{H}_1^{-1}$ is a positive definite diagonal matrix (with $\mathbf{Q} \in \Re^{8\times 8}$), then $\dot{V}_2 < 0$. Therefore, the surface $\tilde{\boldsymbol{x}}_{12} = \mathbf{0}$ is attractive, leading $\tilde{\boldsymbol{x}}_{12}$ to converge towards $\boldsymbol{x}_{12}$.

According to equations (18), it can then be deduced that the estimation error $\tilde{\boldsymbol{x}}_3$ of the road profile and its time derivative $\tilde{\boldsymbol{x}}_4$ also converge towards $\mathbf{0}$. The dynamic estimation error of ξ_1 is given by

$$\dot{\tilde{\xi}}_1 = -\mathbf{J}^{-1}\mathbf{R}\tilde{\boldsymbol{\Psi}} - \boldsymbol{\Lambda}_1 \operatorname{sgn}(\tilde{\xi}_1) \tag{24}$$

The force estimation error $\tilde{\boldsymbol{\Psi}}$ is defined by

$$\dot{\tilde{\boldsymbol{\Psi}}} = -\boldsymbol{\chi} - \boldsymbol{\Lambda}_2 \operatorname{sgn}(\tilde{\xi}_1) \tag{25}$$

Consider the Lyapunov function

$$V_1' = \tfrac{1}{2}\tilde{\xi}_1^{\mathrm{T}}\tilde{\xi}_1 + \tfrac{1}{2}\tilde{\boldsymbol{\Psi}}^{\mathrm{T}}\mathbf{P}\tilde{\boldsymbol{\Psi}} \tag{26}$$

where $\mathbf{P} \in \Re^{4\times 4}$ is a diagonal positive matrix.

According to equations (24) and (25), the time derivative of this function gives

$$\begin{aligned} \dot{V}_1' &= \tilde{\xi}_1^{\mathrm{T}}\dot{\tilde{\xi}}_1 + \tilde{\boldsymbol{\Psi}}^{\mathrm{T}}\mathbf{P}\dot{\tilde{\boldsymbol{\Psi}}} \\ &= -\tilde{\xi}_1^{\mathrm{T}}\boldsymbol{\Lambda}_1 \operatorname{sgn}(\tilde{\xi}_1) - \tilde{\xi}_1^{\mathrm{T}}\mathbf{J}^{-1}\mathbf{R}\tilde{\boldsymbol{\Psi}} \\ &\quad -\tilde{\boldsymbol{\Psi}}^{\mathrm{T}}\mathbf{P}\boldsymbol{\chi} - \tilde{\boldsymbol{\Psi}}^{\mathrm{T}}\mathbf{P}\boldsymbol{\Lambda}_2 \operatorname{sgn}(\tilde{\xi}_1) \end{aligned} \tag{27}$$

while, choosing the matrix $\boldsymbol{\Lambda}_2$ components $(\Lambda_{i2}, i = 1, \ldots, 4)$ such that $\Lambda_{i2} < |\mathbf{P}^{-1}\tilde{\boldsymbol{\Psi}}^{\mathrm{T}-1}\tilde{\xi}_1^{\mathrm{T}}\boldsymbol{\Lambda}_1|$ and $\boldsymbol{\chi} = -\tilde{\xi}_1^{\mathrm{T}}\mathbf{J}^{-1}\mathbf{R}\mathbf{P}^{\mathrm{T}}$, equation (27) becomes

$$\dot{V}_1' = -\tilde{\xi}_1^{\mathrm{T}}\boldsymbol{\Lambda}_1 \operatorname{sgn}(\tilde{\xi}_1) < 0 \tag{28}$$

Therefore, the surface $\tilde{\xi}_1 = \mathbf{0}$ is attractive and $\hat{\xi}_1$ converges towards ξ_1.

4 MAIN RESULTS

In this section, some results are given in order to test and validate the approach. The estimated road profile is compared with the profile measured using a longitudinal profile analyser (LPA) developed at LCPC [**22**]. It is equipped with a laser sensor and accelerometer to measure the elevation of the road profile (see Fig. 4).

The model parameters are measured. However, the pneumatic parameters C_1, C_2, and C_3 are not well

Fig. 4 LPA

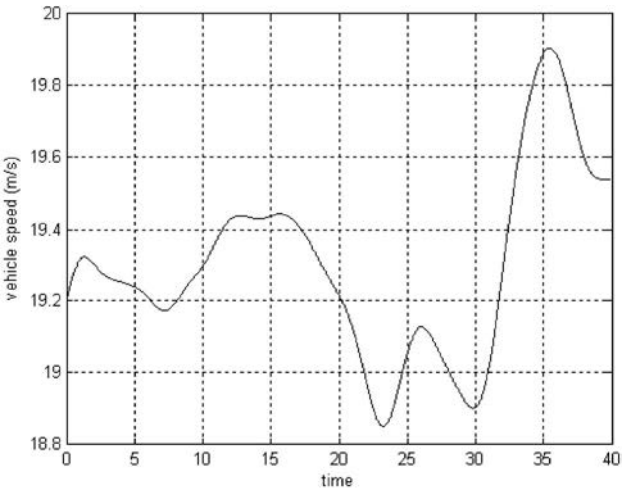

Fig. 5 Vehicle speed

known. To mitigate this disadvantage, observers are used to estimate the longitudinal forces which are related to these parameters. The system outputs are the displacements of the wheels and the chassis, which correspond to signals given by sensors. Different measurements are made with the vehicle moving at several speeds.

Figure 5 shows a vehicle speed average of 70 km/h (20 m/s) with an error which does not exceed 1.2 m/s (Fig. 6).

Figure 7 shows the measured and the estimated displacements. In the upper two plots of Fig. 7 the vertical displacement z and the yaw angle ψ of the chassis are presented. It is shown that these displacements can be estimated rapidly and fairly accurately. The lower two plots of Fig. 7 represent the velocities. It can be seen that the estimated vertical velocity $\dot{z}$ is accurate compared with the true signal.

However, an error occurs concerning the estimation of $\dot{\psi}$. This error is mainly due to sensor calibration (the sensor that was used in the measurements had an error of calibration that could not be corrected).

In Fig. 8, it can be seen that the estimated angular velocity of the wheel converges well towards the actual values in finite time. Indeed, there is a convergence time of only 1 s.

The convergence of the states is very fast and the estimation is of good quality. The good reconstruction of these states allows the unknown inputs to be estimated.

In Fig. 9 the behaviour of the road profile estimator is presented. This figure presents both the measured road profile (measured using the LPA) and the estimated road profile. Thus it can be observed that the estimated values are quite close to the true values. These profiles have the same shape and the differences are not important. Figure 10 shows the power spectral density of the estimated road profile and the profile measured using the LPA.

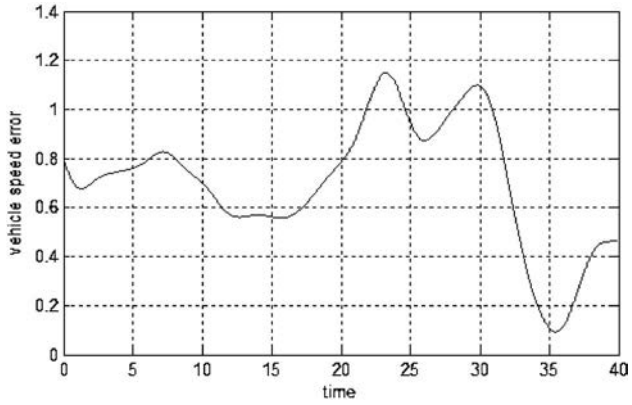

Fig. 6 Vehicle speed error

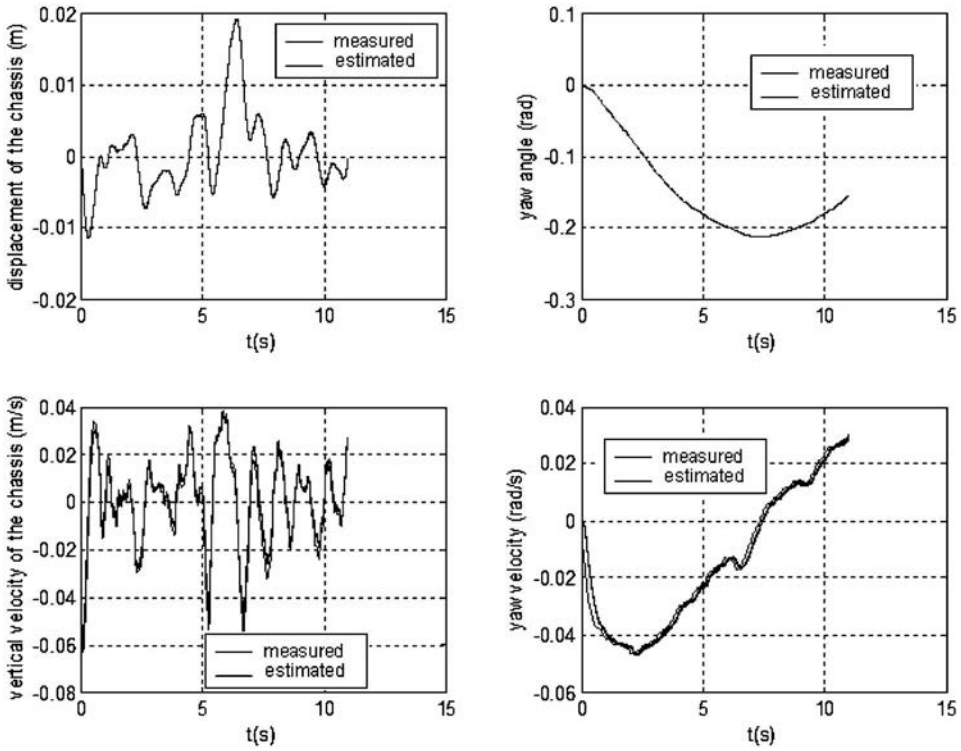

Fig. 7 Estimated and measured states

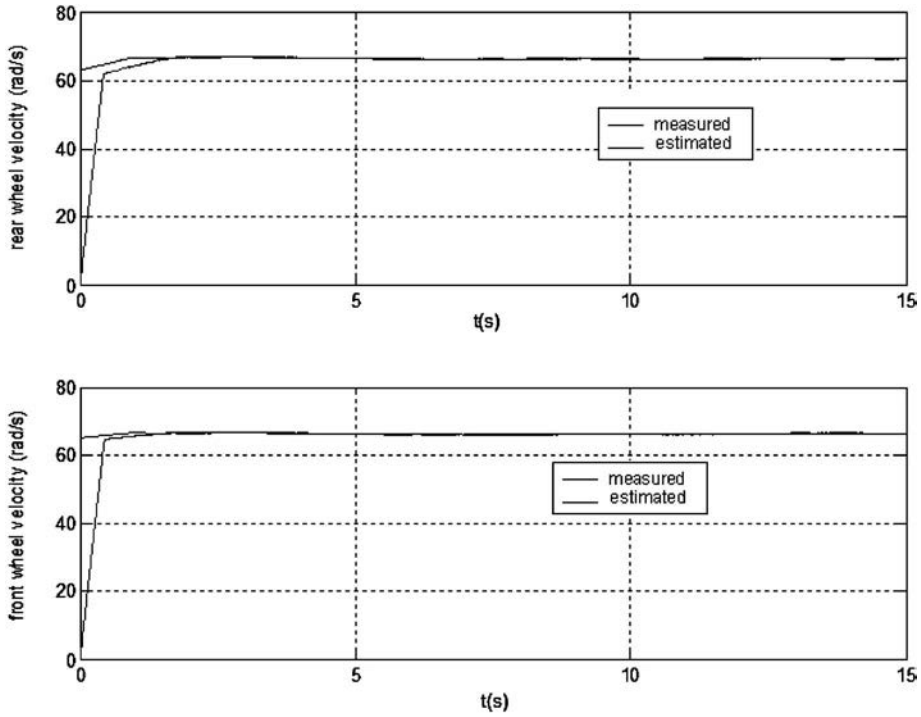

Fig. 8 Estimated and measured wheel velocities

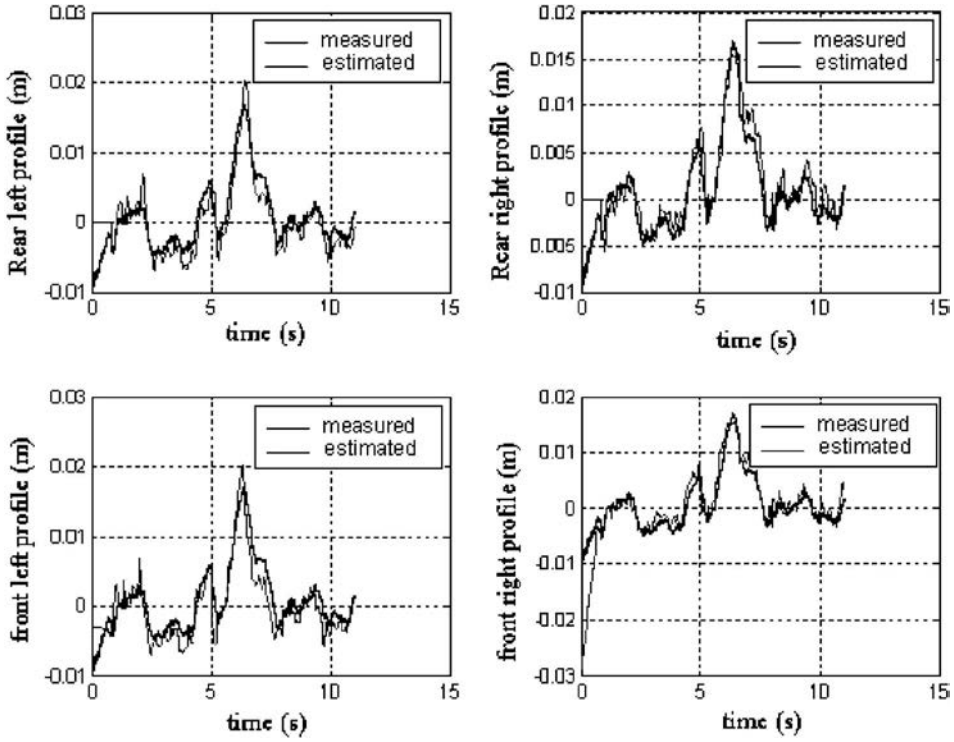

Fig. 9 Comparison of the profile measured using the LPA estimated profile

It should be noted that low and average waves of the road (i.e. mean high and average frequencies) respectively are well reconstructed. However, there are limitations of this method in estimating high waves of the road.

5 CONCLUSION

In this paper, sliding-mode observers have been developed to estimate the longitudinal tyre–road forces of the system and the unknown inputs which

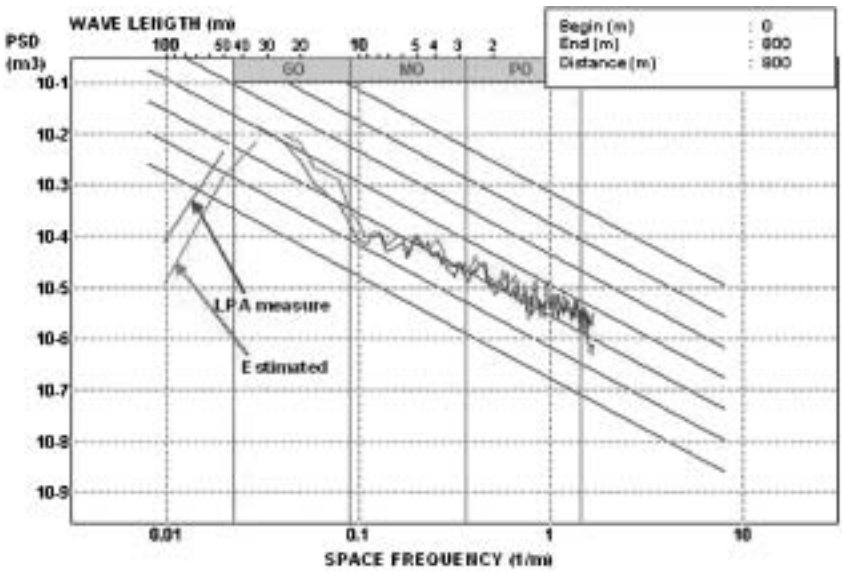

Fig. 10 Power spectral density (PO, low wave; MO, average wave; GO, high wave)

correspond to the road profile. The parameters of the system are presumably measured and known. However, the pneumatic coefficients which intervene in the calculation of the longitudinal forces are unknown. This is why another observer was built to consider directly these longitudinal forces. It was observed that the profile estimated by this approach is very close to that measured using the LPA. However, local variations appear. It is then important to know whether these variations penalize the capability of these profiles (of bandwidth broader than the LPA) to determine the dynamic response of vehicle (previous studies have shown that the profile measured by the LPA is not correct for considering this dynamic response). In the continuation of this work, these profiles will be considered as inputs of the dynamic model of the vehicle to estimate the instantaneous loads of the wheels. Thus the dynamic responses measured on an instrumented vehicle can be compared with those estimated by simulation of the vehicle.

REFERENCES

1 **Van Der Jagt, P.** and **Parson, A.** Road surface correction of tire test data. In Proceedings of the First International Colloqium on *Tyre Models for Vehicles Dynamics Analysis*, Delft, The Netherlands, 21–22 October 1991.

2 **Misum** Simulation of the interaction between vehicle wheel and the unevenness of the road surface. *Veh. System Dynamics*, 1990, **19**, 237–253.

3 **Harrison, R. F.** The non-stationary response of vehicles on rough ground. PhD thesis, Institute of Sound and Vibration Research Faculty of Engineering and Applied Science, University of Southampton, 1983.

4 **Pong, M.-F. M.** The development of an extensive-range dynamic road profile and roughness measuring system. May 1992.

5 **Karunasena, W. G.** Determination of road roughness from inertial profilometer data. PhD theses, The Pennsylvania State University, University Park, Pennsylvania, USA, 1984.

6 **Spangler, E. B.** and **Kelly, W. J.** GMR road profilometer method for measuring road profile. Publication GMR-452, General Motors Research, 1964.

7 **Gillespie, T. D.** *et al.* Methodology for road roughness profiling and rut depth measurement. Report FHWA/RD-87-042, Federal Highway Administration, 1987, 50 pp.

8 **Imine, H., M'Sirdi, N. K.,** and **Delanne, Y.** Adaptive observers and estimation of the road profile. In Proceedings of the SAE World Congress, Detroit, Michigan, USA, March 2003, pp. 175–180 (Society of Automotive Engineers, New York).

9 **Barbot, J. P., Boukhobza, T.,** and **Djemai, M.** Triangular input observer form and sliding mode observer. In Proceedings of the 35th IEEE Conference on *Decision and Control*, Kobe, Japan, 1996, pp. 1489–1491 (IEEE, New York).

10 **Bestle** and **Zeitz** Canonical form observer design for nonlinear time varying systems. *Int. J. Control*, 1988, **47**, 1823–1836.

11 **Drakunov, S. V.** Sliding-mode observers based on equivalent control method. In Proceedings of the 31st IEEE Conference on *Decision and Control*, Tucson, Arizona, USA, 1992, pp. 2368–2369 (IEEE, New York).

12 **Xia, X.** and **Gao, W.** Nonlinear observer design by observer error linearization. *SIAM J. Control Optimization*, 1989, **27**(1), 199–213.

13 **Mendoza** Sur la modèlisation et la commande des véhicules automobiles. Thèse de Doctorat, Institut National Polytechnique de Grenoble, Grenoble, France, 22 July.

14 **Canudas, C.** and **Horowitz, R.** Observer for tire road contact friction using only wheel angular velocity information. In Proceedings of the 38th IEEE Conference on *Decision and Control*, Phoenix, Arizona, USA, 1999 (IEEE, New York).

15 **Bakker, E., Pacejka, H. B.,** and **Linder, L.** A new tire model with an application in vehicle dynamics studies. *SAE Trans.*, 1989, **98**(6), 101–113.

16 **Burckhardt, M.** *Fahrwerktechnik, Radschlupfregelsysteme*, 1993 (Vogel-Verlag, Würzburg).

17 **Xiong, Y.** and **Saif, M.** Sliding mode observer for nonlinear uncertain systems. *IEEE Trans. Autom. Control*, 2001, **46**(12), 2012–2017.

18 **Hostetter, G.** and **Meditch, J. S.** Observing systems with unmeasurable inputs. *IEEE Trans. Autom. Control*, June 1973, **18**, 307–308.

19 **Johnson, C. D.** On observers for systems with unknown and inaccessible inputs. *Int. J. Control*, 1974, **21**(5), 825–831.

20 **Yang, H.** and **Saif, M.** Fault detection in a class of nonlinear systems via adaptive sliding observer design. In Proceedings of the IEEE Conference on *Systems, Man and Cybernetics*, 1995, pp. 2199–2204 (IEEE, New York).

21 **Utkin, V. I.** and **Drakunov, S.** Sliding mode observer. In Proceedings of the 34th IEEE Conference on *Decision and Control*, New Orleans, Lousiana, USA, 1995, pp. 3376–3378 (IEEE, New York).

22 **Legeay, V., Daburon, P.,** and **Gourraud, C.** Comparaison de mesures de l'uni par analyseur de profil en long et par compensation dynamique. Bulletin Interne, Laboratoire Central des Ponts et Chaussées, DGER–IRVAR, December 1994.